THE JOURNAL OF BIOLOGICAL CHEMISTRY VOL. 290, NO. 20, pp. 12899–12907, May 15, 2015

Baicalin Inhibits the Lethality of Ricin in Mice by Inducing Protein Oligomerization*

Received for publication, December 17, 2014, and in revised form, April 1, 2015 Published, JBC Papers in Press, April 5, 2015, DOI 10.1074/jbc.M114.632828

Jing Dong[‡§1], Yong Zhang[‡1], Yutao Chen[¶1], Xiaodi Niu[‖], Yu Zhang[‡], Rui Li[‡], Cheng Yang[**], Quan Wang[¶], Xuemei Li[¶2], and Xuming Deng[‡3]

*From the [‡]Key Laboratory of Zoonosis, Ministry of Education, Institute of Zoonosis, College of Veterinary Medicine, Jilin University, Changchun 130062, the [§]Yangtze River Fisheries Research Institute, Chinese Academy of Fishery Sciences, Wuhan 430223, the [¶]National Laboratory of Biomacromolecules, Institute of Biophysics, Chinese Academy of Sciences, Beijing 100101, the [‖]Department of Food Quality and Safety, Jilin University, Changchun 130062, and the **College of Pharmacy, NanKai University, Tianjin 300071, China*

Background: Ricin is known as a potential bioterrorism agent without efficacious therapeutic treatments.
Results: Baicalin can inhibit the activity of ricin both *in vitro* and *in vivo* by inducing ricin to form oligomers.
Conclusion: The protective effect is better than antibodies and other inhibitors.
Significance: This work offers promising leads for the development of therapeutics against ricin.

Toxic ribosome-inactivating proteins abolish cell viability by inhibiting protein synthesis. Ricin, a member of these lethal proteins, is a potential bioterrorism agent. Despite the grave challenge posed by these toxins to public health, post-exposure treatment for intoxication caused by these agents currently is unavailable. In this study, we report the identification of baicalin extracted from Chinese herbal medicine as a compound capable of inhibiting the activity of ricin. More importantly, post-exposure treatment with baicalin significantly increased the survival of mice poisoned by ricin. We determined the mechanism of action of baicalin by solving the crystal structure of its complex with the A chain of ricin (RTA) at 2.2 Å resolution, which revealed that baicalin interacts with two RTA molecules at a novel binding site by hydrogen bond networks and electrostatic force interactions, suggesting its role as molecular glue of the RTA. Further biochemical and biophysical analyses validated the amino acids directly involved in binding the inhibitor, which is consistent with the hypothesis that baicalin exerts its inhibitory effects by inducing RTA to form oligomers in solution, a mechanism that is distinctly different from previously reported inhibitors. This work offers promising leads for the development of therapeutics against ricin and probably other ribosome-inactivating proteins.

As important members of the ribosome-inactivating protein (RIP)[4] family, ricin is an RNA *N*-glycosidase that specifically cleaves a conserved adenosine residue in 28S rRNA, leading to the arrest of protein synthesis and subsequent killing of eukaryotic cells (1). Although ricin toxicosis is not a disease, several severe injuries both in human and animal models can develop after administration of ricin. Death caused by ricin can take up to 4–5 days, but no efficacious therapeutic treatments are available (2). The LD_{50} value of ricin holotoxin of about 1 μg/kg of body weight for mice, rats, and dogs and depending on the mode of administration, the lethal dose to human is in the 0.1–1.0 μg/kg range (3). Because it is relatively easy to obtain large quantities, ricin is a potential bioterrorism agent, thus posing a grave challenge to public health (4).

Ricin is an AB-type toxin consisting of a catalytic A subunit (RNA *N*-glycosidase) (RTA) and B subunit(s) important for entering cells. Internalization of ricin is mediated by the binding of its B subunit (RTB) as the galactose/*N*-acetylgalactosamine (Gal/GalNac)-specific lectin (5). Once inside the cells, the vesicle containing the toxin is delivered via the retrograde transport pathway to the endoplasmic reticulum. The toxin finally reaches the cytoplasm from the endoplasmic reticulum by retro-translocation and imposes its effects on the ribosome substrate (6), which can inhibit protein synthesis by removing an adenine at position 4324 in the sarcin/ricin domain of 28S rRNA of the 60S ribosomal subunit (7).

Antibodies and small molecular inhibitors are currently being developed for post-exposure measures against these toxins (8). A number of ricin-specific murine monoclonal antibodies (mAbs) have been reported (9–11). Among these, several ricin-specific mAbs have been humanized and used in clinical trials (12–14). Despite this progress, it is worth noting that only a few of these mAbs have been shown to effectively treat conditions caused by ricin after intoxication has occurred (15, 17). Similarly, few clinically effective small molecular inhibitors

* This work was supported by National Basic Research Program of China Grant 2013CB127205 (to X. M. D.), National Nature Science Foundation of China Grant 31130053 (to X. M. D.), and National 863 Program of China Grant 2012AA020303 (to X. M. D.).
The atomic coordinates and structure factors (code 4Q2V) have been deposited in the Protein Data Bank (http://wwpdb.org/).
[1] These authors contributed equally to this work.
[2] To whom correspondence may be addressed: National Laboratory of Biomacromolecules, Institute of Biophysics, Chinese Academy of Sciences, Beijing 100101, China. Tel.: 86-010-64888554; E-mail: lixm@sun5.ibp.ac.cn.
[3] To whom correspondence may be addressed: Key Laboratory of Zoonosis, Ministry of Education, Institute of Zoonosis, College of Veterinary Medicine, Jilin University, Changchun 130062, China. Tel.: 86-0431-87836161; E-mail: dengxm@jlu.edu.cn.

[4] The abbreviations used are: RIP, ribosome-inactivating protein; BAI, baicalin; RTA, a chain of ricin; LDH, lactate dehydrogenase; PDB, Protein Data Bank.

TABLE 1
Primers used for introducing the mutations

Primers	Sequence (5′ to 3′)
RTA-R189A-F	GAGGGAGAAATG**GCG**ACGAGAATTAG
RTA-R189A-R	CTAATTCTCGT**CGC**CATTTCTCCCTC
RTA-T190A-F	GGGAGAAATGCGC**GCG**AGAATTAGGTAC
RTA-T190A-R	GTACCTAATTCT**CGC**GCGCATTTCTCCC
RTA-R193A-F	GCACGAGAATT**GCG**TACAACCGGAG
RTA-R193A-R	CTCCGGTTGTA**CGC**AATTCTCGTGC
RTA-Y194A-F	CGAGAATTAGG**GCG**AACCGGAGATC
RTA-Y194A-R	GATCTCCGGTT**CGC**CCTAATTCTCG
RTA-R235A-F	CAATTCAACTGCAAAGA**GCG**AATGGTTCCAAATTCAG
RTA-R235A-R	CTGAATTTGGAACCATT**CGC**TCTTTGCAGTTGAATTG
RTA-R258A-F	GCTCTCATGGTGCAT**GCG**TGCGCACCTCCACC
RTA-R258A-R	GGTGGAGGTGCGCA**CGC**ATGCACCATGAGAGC

against this toxin have been identified. One compound has been shown to significantly protect mice against ricin challenge (18), but its therapeutic effects remain unknown.

In this study, we identified baicalin (BAI), a compound extracted from traditional Chinese herbal medicine, as an effective therapeutic against ricin via a novel mechanism. BAI functions by inducing the formation of oligomers by RTA, which results in the loss of the *N*-glycosidase activity of the toxin. BAI may be used as a promising candidate for the treatment of ricin.

EXPERIMENTAL PROCEDURES

Chemicals and Reagents—BAI was purchased from Sigma, and the stock solutions were prepared in dimethyl sulfoxide (DMSO) (Sigma). For animal experiments, BAI was dissolved in sterile PBS.

Isolation and Purification of Ricin—Ricin holotoxin was extracted and purified from seeds of castor bean (*Ricinus communis*) as described (19). Briefly, crude toxin was extracted using ammonium sulfate precipitation and then the toxin was applied to a *p*-aminobenzyl 1-thio-β-D-galactopyranoside-agarose column and washed with PBS buffer; ricin and agglutinin were eluted with 0.5 M galactose. Ricin was separated from agglutinin using a Superdex 75 column (19). After dialyzing against PBS buffer, ricin was stored at −80 °C.

Expression and Purification of RTA and Its Mutants—The cDNA encoding WT-RTA protein was amplified using genomic DNA of *R. communis* seeds as template. Two restriction endonuclease sites (BamHI and XhoI) were attached to the 5′ ends of the primers to facilitate subsequent cloning. The purified PCR product was digested with BamHI and XhoI overnight and cloned into the pGEX-6P-1 expression vector (Merck) that had been treated with the same enzymes, resulting in the recombinant plasmid pGEX-6P-1-*rta*. The mutations were introduced by site-directed mutagenesis, and all mutations were verified by double strand DNA sequencing. Primers used for introducing the mutations are listed in Table 1.

RTA and its mutants were expressed in *Escherichia coli* BL21(DE3) in LB medium. Protein expression was induced by 1 mM IPTG (final concentration) when the cultures grew to an A_{600} of ~0.6, and the induction was allowed to proceed for 6 h at 37 °C. Cells harvested by centrifugation were lysed by sonication in PBS buffer, and the insoluble fraction was removed by 30 min of centrifugation at 18,000 × *g* at 4 °C. Cleared supernatant was loaded into 2-ml affinity column of self-packed GST beads (GE Healthcare). The column was washed with 200 ml of washing buffer (lysis buffer with 200 mM NaCl). The bead-GST-RTA complex was incubated with PreScission protease (GE Healthcare) at 4 °C overnight to remove the GST tag. Full-length RTA protein with 5 extra residues (GPLGS) in the N-terminal end was eluted with the lysis buffer. The protein was then desalted by passing through a Sephadex G-25 column (GE Healthcare). The desalted sample was purified using a HiTrap Q 1-ml column (GE Healthcare) with 25 mM glycine, pH 9.4, 0–1 M NaCl; protein was further purified using a Superdex 75 16/60 column (GE Healthcare) on an AKTA system. Fractions containing target protein were pooled and stored at −80 °C for subsequent applications.

Cell Free Translation Assay—TnT®-coupled reticulocyte lysate systems and luciferase assay systems (Promega, Madison, WI) were used to measure the toxicity of ricin in protein synthesis. 10 ng of ricin (20) and BAI ranging from a concentration of 9 μM to 72 μM were added to the reaction system according to the manufacturer's directions. After incubation for 90 min at 30 °C in a water bath, the reaction was terminated by placing the plates on ice and analyzed by the luciferase assay system.

Cell Based Assay for Protection against Ricin—HeLa cells were cultured in Dulbecco's modified Eagle's medium (DMEM) supplemented with 3 mM glutamine, antibiotics (100 units/ml penicillin and 100 units/ml streptomycin), 10% heat-inactivated fetal bovine serum, at 37 °C in 5% CO_2 in a humidified incubator. For the assay, HeLa cells were plated into 96-well plates at a density of 1.5×10^4 cells per well in DMEM and incubated for 16 h at 37 °C in 5% CO_2. The cells were incubated with 1 ng/ml ricin (capable of killing about 80% of cells as determined in pilot experiments) with BAI at different concentrations for 72 h at 37 °C. Negative controls without toxin were similarly established. Cell viability was evaluated by lactate dehydrogenase (LDH) release using a cytotoxicity detection kit (LDH) (Roche Applied Science) according to the manufacturer's directions. Plates were read on a microplate reader (TECAN, Austria) at 490 nm. To measure the effect of baicalin on cell viability, cells were incubated with various concentrations of the compound for 2 h, and viability was then evaluated spectrophotometrically at 490 nm using the nonradioactive cell proliferation assay kit (Promega, Madison, WI) following the manufacturer's instructions.

Mice Injection Protocols—All animal studies were performed according to the Regulations for the Administration of Affairs Concerning Experiments Animals (1988.11). The experimental protocols were approved and supervised by the Institutional Animal Care and Use Committee (IACUC) of Jilin University.

For lethality assay, 8-week-old BALB/c mice weighing 16–18 g obtained from the Experimental Animal Center of Jilin University (Changchun, China) were injected intraperitoneally with 100 μl of sterile PBS or ricin. For mortality studies, mice were administered ricin at a single dose of 500 ng per mouse (~2 × LD_{50}). 6 h after injection, the infected mice were administered 100 mg/kg BAI subcutaneously and then at 6-h intervals. Mice were weighed every day after infection.

Measurement of Blood Glucose—For measurement of blood glucose, mice were euthanized, and blood samples were taken from the saphenous vein 72 h after injection. Blood glucose

TABLE 2
Data collection statistics

Parameters	Ricin-baicalin complex
Space group	$P4_12_12$
Resolution range[a]	50–2.20 (2.24–2.20)
Cell dimensions (Å)	
A	68.2
B	68.2
C	133.3
Total no. of reflections	155,524
No. of unique reflections	16,723
Completeness (%)[a]	99.9 (100.0)
Redundancy[a]	9.3 (9.6)
$I/\sigma(I)$[a]	34.4 (5.3)
R_{merge} (%)[a,b]	7.5 (47.6)

[a] Values in parentheses correspond to the shell of highest resolution.
[b] $R_{merge} = \sum_{hkl}|I_i - I_m|/\sum_{hkl}\langle I_m\rangle$, where I_i and I_m are the observed and mean intensity of related reflections with common indices *h, k,* and *l*.

TABLE 3
Structure refinement statistics

Parameters	Ricin-baicalin complex
No. of reflections in working set	15,826
No. of reflections in test set	842
R_{work}[a]	0.211
R_{free}[a]	0.243
Root mean square deviation	
Bond lengths (Å)	0.009
Bond angles (°)	1.052
Average B factors (Å^2)	
Total	46.2
Ricin	46.0
Baicalin	57.5
Solvent	44.2
Residues in Ramachandran plot (%)	
Favored	97.7
Allowed	2.3
Disallowed	0.0

[a] $R_{work} = \sum\|F_{obs}|-|F_{cal}\|\sum F_{obs}|$ and $R_{free} = \sum_T\|F_{obs}|-|F_{cal}\|/\sum_T|F_{obs}|$, where F_{obs} and F_{cal} are observed and calculated structure factors, respectively. For R_{free}, T is a randomly selected test data set (5.0%) of total reflections and was set aside before structure refinement.

level was determined by use of a handheld glucometer (AccuChek Advantage, Roche Diagnostics).

Cytokine Detection in Livers—Livers were dissected from mice with different treatment 72 h after injection. Livers were placed in PBS buffer and homogenized using a tissue homogenizer. Following centrifugation, supernatants were collected and stored at −20 °C until analysis. Cytokine levels were measured using an enzyme-linked immunosorbent assay (ELISA) by specific mouse ELISA kits (BioLegend).

Crystallization of RTA-Inhibitor Complexes—Purified RTA in a buffer (75 mM Tris-HCl, pH 8.9, 10 mM β-mercaptoethanol, 1 mM EDTA) was concentrated to about 4 mg/ml using an Ultrafree-15 centrifugal filter (Millipore). Initial crystal screening was performed at 16 °C in 96-well plates by the hanging-drop vapor diffusion method using the sparse matrix screening kits from Hampton Research, followed by a refinement of the conditions through the variation of precipitant, pH, protein concentration, and chemical additives. In particular, 2-μl droplets were prepared on siliconized coverslips by mixing 1 μl of protein solution (4 mg/ml) and 1 μl of the reservoir solution (0.2 M ammonium sulfate, 0.1 M sodium acetate, pH 4.6, 10% (w/v) PEG 4000) before equilibrating against 200 μl of the reservoir solution. The compound BAI was dissolved in the RTA stock solution at 10 mM and soaked into RTA crystals. After soaking for 7 days, the crystals were mounted for x-ray data collection.

X-ray Diffraction Data Collection and Structure Determination—The BAI-soaked RTA crystals was harvested from the drop and briefly soaked for 5 s in a cryo-protectant containing the reservoir solution and 15% glycerol before being mounted for x-ray diffraction. Crystals with the highest resolution were flash-frozen in liquid nitrogen before diffraction data were collected at Beamline 17U of the Shanghai Synchrotron Radiation Facility at 100 K. Data were processed using the HKL2000 program package (21), and relevant statistics were summarized in Table 2. The soaked crystals were in the same space group of $P4_12_12$, with very close cell dimensions as to the native RTA crystals.

We used the crystal structure of RTA (PDB code 1J1M) as the search model and program Phaser (22) was applied to solve the crystal structure of the RTA-BAI complex. The structure of the BAI molecule was placed and modeled by the guidance of the $F_o - F_c$ electron density map, where F_o and F_c are the observed and calculated structure factors, respectively. Automatic and manual adjustment and refinement were carried out with crystallographic programs REFMAC (23), Phenix (24), and COOT (25). At the final stage, water molecules were added to the $F_o - F_c$ map peaks ($\sigma > 2.5$) where they could form reasonable hydrogen bonds with nearby amino acid residues. The final refined RTA-BAI crystal structure was validated by program PROCHECK (26), with no residue located at the disallowed region of the Ramachandran plot, and statistics for structure refinement have been summarized in Table 3. Structural analysis was performed by program EdPDB, and structure figures were generated by PyMOL (DeLano Scientific LLC). The coordinates and structure factors of RTA-ricin complex structure was deposited in Protein Data Bank with the PDB code 4Q2V.

Analytical Ultracentrifugation—Sedimentation velocity analysis was performed on a Beckman XL-I analytical ultracentrifuge at 20 °C. Protein samples were diluted with RTA buffer to 400 μl at an $A_{280\ nm}$ absorption of about 0.70; BAI was preincubated with protein samples at a molar ratio of about 300:1 for 30 min. Samples were loaded onto a conventional double-sector quartz cell and mounted in a Beckman four-hole An-60 Ti rotor. Data were collected at 262,000 × *g* at a wavelength of 280 nm. Interference sedimentation coefficient distributions were calculated from the sedimentation velocity data using the SEDFIT software program.

Statistical Analysis—When necessary, the experimental data were analyzed by the independent Student's *t* test with SPSS 14.0 statistical software (SPSS Inc., Chicago, IL), and a *p* value less than 0.05 was considered to be statistically significant. The statistical analysis for survival was measured by the log rank test.

RESULTS

Baicalin Inhibits the Toxicity of Ricin to Cultured Cells—To identify natural compounds capable of inhibiting the toxicity of RIPs, we initiated a cell-based assay (27) to screen chemicals extracted from Chinese herbal medicine. Purified ricin (purity

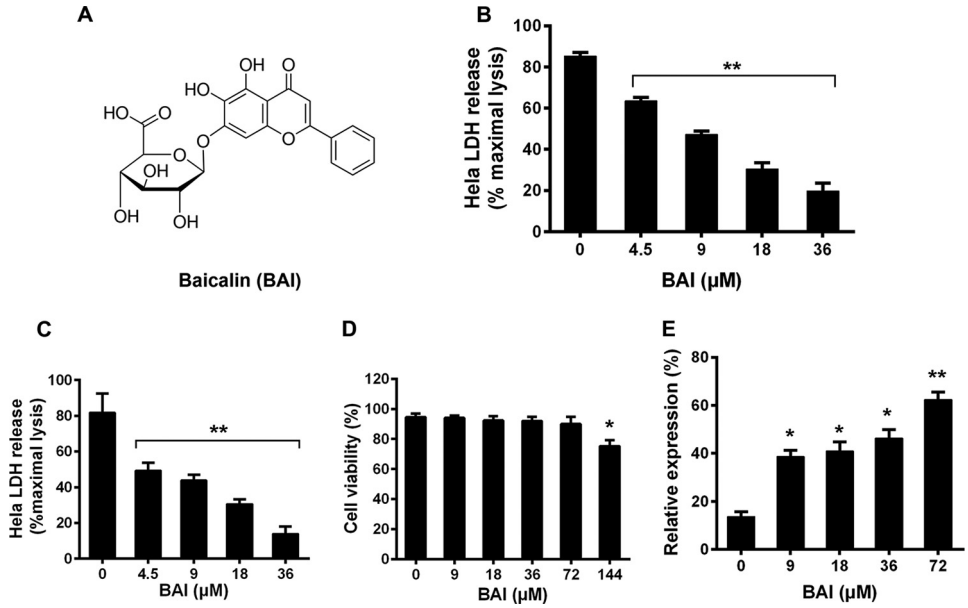

FIGURE 1. **Inhibitory effect of baicalin against ricin.** *A,* chemical structure of baicalin. *B,* inhibition of cell death by baicalin. Ricin was added into HeLa cells treated with the indicated concentrations of baicalin for 72 h. Cell viability was evaluated by measuring extracellular LDH 72 h after adding the toxins. *C,* ricin premixed with baicalin exhibited lower toxicity. Ricin mixed with the indicated amounts of baicalin was added to HeLa cells, and the release of LDH was measured after incubating for 72 h. *D,* effects of baicalin on cell viability. HeLa cells were treated with the indicated concentrations of baicalin for 2 h before viability was determined. *E,* effects of baicalin on the inhibition of protein synthesis by ricin. Baicalin was added to reactions for *in vitro* protein synthesis with ricin, and the expression of luciferase mRNA was measured. All data represent the mean and standard error of three independent experiments. *, $p < 0.05$; **, $p < 0.01$.

>90%) was added to HeLa cells pretreated with the testing molecules, and the toxicity was evaluated by the release of LDH. We found that baicalin (BAI, Sigma, purity >95%) (Fig. 1*A*), a flavonoid from the Chinese medicinal herb Huang-chin (*Scutellaria baicalensis*), is able to effectively protect ricin-induced cell death (Fig. 1*B*). Further analysis indicated that pretreatment with as little as 4.5 μM BAI was able to significantly inhibit cell death induced by ricin. We also detected similar alleviation of the toxicity when a mixture of BAI and ricin was applied to the cells (Fig. 1*C*), suggesting that this compound may directly target the toxins. At concentrations sufficient for significantly inhibiting the toxicity, BAI exerted negligible effects on cell viability; significant inhibition only was observed when 144 μM was incubated with HeLa cells (Fig. 1*D*). Ricin induces cell death by targeting protein synthesis; we thus examined the effects of BAI on this activity using a cell-free translation system with luciferase as readout. In reactions containing 10 ng of ricin ($\sim 2 \times IC_{50}$), as low as 9 μM BAI significantly rescued the translation inhibition imposed by ricin (Fig. 1*E*). We found that the translation was restored to ~60% of the toxin-free controls when 72 μM of the compound was included in the reactions (Fig. 1*E*). These results indicate that BAI is capable of neutralizing the toxicity of ricin by interfering with its inhibitory effects on protein synthesis.

BAI Therapeutically Prevents the Lethality Induced by Ricin in Mice—Given the effectiveness of BAI in *in vitro* inhibition of the activity of ricin, we investigated the usefulness of this compound in the protection of animals exposed to the toxin (under our experimental conditions, the LD_{50} value of ricin is about 250 ng/mouse). A mouse model in which the toxin was administered by intraperitoneal injection was used. Under our experimental condition, a single dose of ricin ($\sim 2 \times LD_{50,}$ 500 ng) led to 100% deaths within 6 days (Fig. 2*A*). These animals started to exhibit signs of tremors and ataxia 2 days after receiving the toxins, and death began to occur on the 3rd day (Fig. 2*A*). After testing several doses ranging from 50 to 300 mg/kg, we found that mice could be effectively protected by BAI at 100 mg/kg, which was then chosen for further experiments. In animals that received BAI subcutaneously, 100 mg/kg 6 h post-exposure and subsequently at 6-h intervals during the entire experimental duration, significant protection was achieved in animals exposed to ricin, in which 50% of the animals survived (Fig. 2*A*). These results established that BAI could provide effective therapeutic protection against lethality caused by ricin.

We further evaluated the therapeutic effects of BAI against the weight loss symptom associated with ricin. Mice injected with PBS or a single dose of ricin (500 ng per mouse) were monitored for body weight at 24-h intervals. In the treated group, 100 mg/kg BAI was administered 6 h after toxin injection and subsequently at 6-h intervals. As expected, in control mice receiving a saline solution, the body weight remained constant during the entire experimental duration (Fig. 2*B*). In contrast, in the group injected with the toxin, the animals exhibited decreased food and water intake. Weight loss became apparent in 2 days, and the mice appeared to regain the weight after reaching the lowest point on the 4th day (Fig. 2*B*); then all the mice in the group injected with ricin died on the 5th day. Treatment with BAI delayed the occurrence of the weight loss for about 24 h; furthermore, the symptom was significantly less severe in the entire experimental duration (Fig. 2*B*).

Treatment with BAI Improves Blood Glucose and Cytokine Release in Liver as Induced by Ricin—To determine whether mice were protected against ricin after administering BAI, we measured the blood glucose level after ricin challenge with or

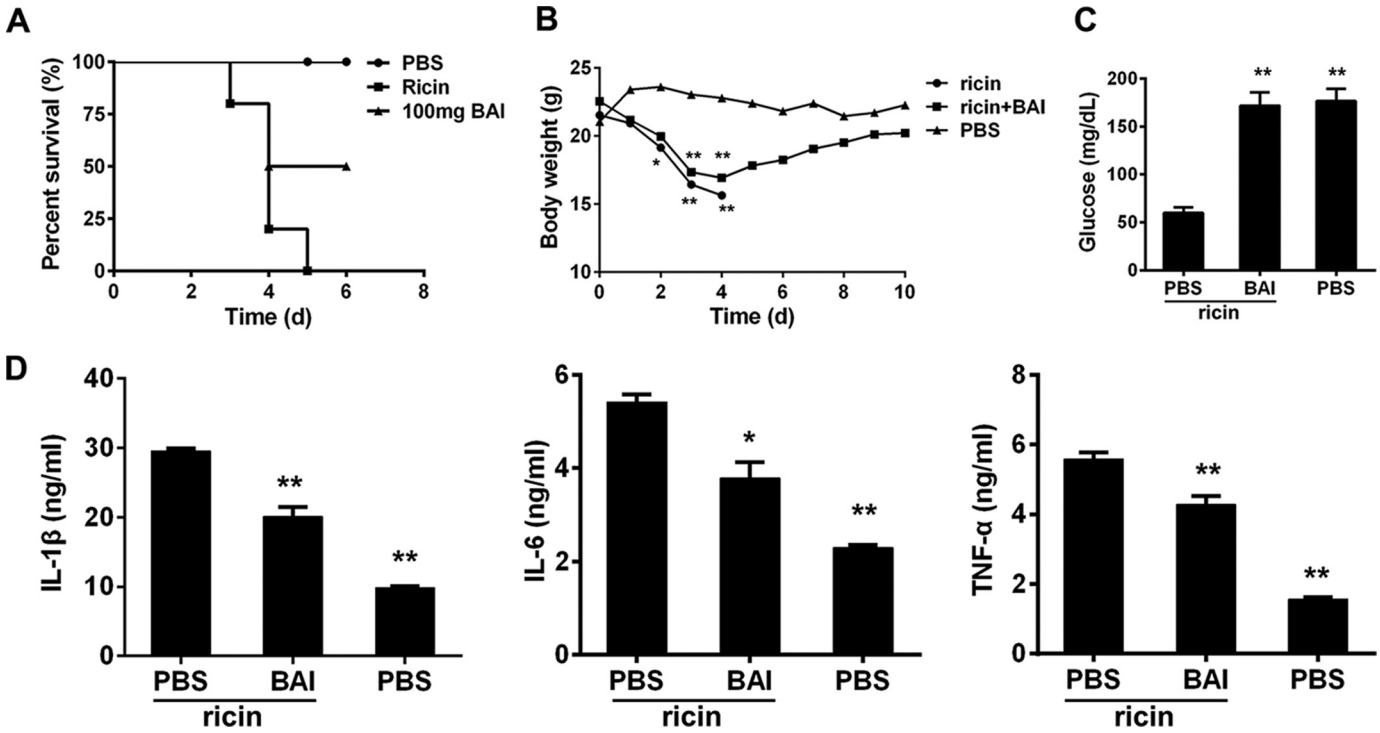

FIGURE 2. **Treatment with baicalin alleviated the pathologies induced by ricin.** *A,* baicalin protects mice against lethality caused by ricin. Groups ($n = 10$) of mice injected with ricin were treated with saline solution or with BAI 6 h post-toxin injection as described under "Experimental Procedures," and the survival of the animals was monitored for 6 days (*d*). The death of mice was followed up to 6 days after ricin injection with no additional mortalities shown in the figure. The curves for treated mice with BAI are statistically different from ricin-injected mice as evaluated by the log rank test, $p = 0.0001$ for 100 mg/kg BAI against ricin. *B,* effects of BAI on body weight caused by ricin. Groups ($n = 10$) of mice injected with ricin or control solution were administered with BAI or PBS 6 h post-toxin injection. The body weight was monitored daily for 10 days. Similar results were obtained from more than three independent experiments; *, $p < 0.05$; **, $p < 0.01$. *C,* effect of BAI on blood glucose level induced by ricin. The levels of blood glucose were evaluated at 72 h after treatment; $n = 5$; *, $p < 0.05$; **, $p < 0.01$. *D,* baicalin reduced the production of several cytokines induced by ricin in liver. Liver tissues from relevant mice were measured for cytokines by ELISA. Note the reduction of cytokine production after baicalin treatment; $n = 5$; *, $p < 0.05$; **, $p < 0.01$.

without BAI administration at 72 h after injection. The blood glucose level in mice receiving ricin alone decreased to 60.05 ± 13.25 mg/dl, which was significantly lower than that from BAI-treated mice (171.90 ± 31.02 mg/dl). Indeed, this level is comparable with 176.72 ± 28.23 mg/dl observed in control mice never injected with ricin (Fig. 2*C*).

We also examined the level of several relevant cytokines to determine whether BAI reduces inflammation accompanied by liver damage. As expected, ricin caused elevated IL-1β, IL-6, and TNF-α (Fig. 2*D*). Consistent with its effect in protecting liver damage, the levels of these cytokines significantly decreased in mice treated with BAI (Fig. 2*D*). Taken together, these results indicated that BAI effectively reduced the damage to the liver caused by ricin.

Baicalin Induces the A Subunit of Ricin to Form Oligomers—Our observation on the protective effects of BAI against ricin suggests that this compound exert its protection by directly targeting the toxin. To fully understand its mechanism of action, we sought to determine the structure of the complex formed by BAI and the RTA of ricin. High resolution structure of the RTA has allowed direct visualization of its active site (Fig. 3*A*) (28). Because high concentrations of BAI have been proved to interfere with the crystallization of the RTA in our previous experiment, we resorted to the soaking method to obtain crystals of the complex by incubating pre-formed RTA crystals in freshly prepared reservoir solution containing 10 mM BAI. After soaking in BAI for 7 days, the crystals remained isomorphous, which had the same space group of $P4_12_12$ as the native ones. Furthermore, crystals of the complex diffracted well, which allowed us to solve its structure at a 2.2 Å resolution by the molecular replacement method. Because of the lack of interpretable electron density maps at both the N- and C-terminal ends of the protein, the final structure contains residues 5–263 (Fig. 3*B*). In its complex with BAI, the RTA molecule retained identical structure to its native form (PDB code 1J1M), with a root mean square deviation of 0.367 Å.

In the structure, the BAI molecule is positioned in the highly positively charged interface of two RTA molecules, which were related by a crystallographic 2_1 helical axis (Fig. 3*B*). The two identical monomers formed a buried surface area of about 700 Å^2, indicative of only moderate packing interactions between these two monomers. In the dimer form, the formation of the oligomers linked by BAI blocked the entry to the active site of one monomer (Fig. 3*B*). If oligomers were formed, the number of active sites accessible by the substrate will be drastically reduced. The structure also indicated that the binding pocket for BAI in the complex was formed by Arg-189, Thr-190, Arg-193, Tyr-194, Arg-235, and Arg-258 from both monomers (Figs. 3*C* and 4).

We also calculated the difference Fourier map based on the difference of observed structure factors in x-ray diffraction data between native and BAI-soaked crystals, with calculated phase from correctly placed RTA molecule after molecular replacement calculation. These analyses unambiguously indicated the

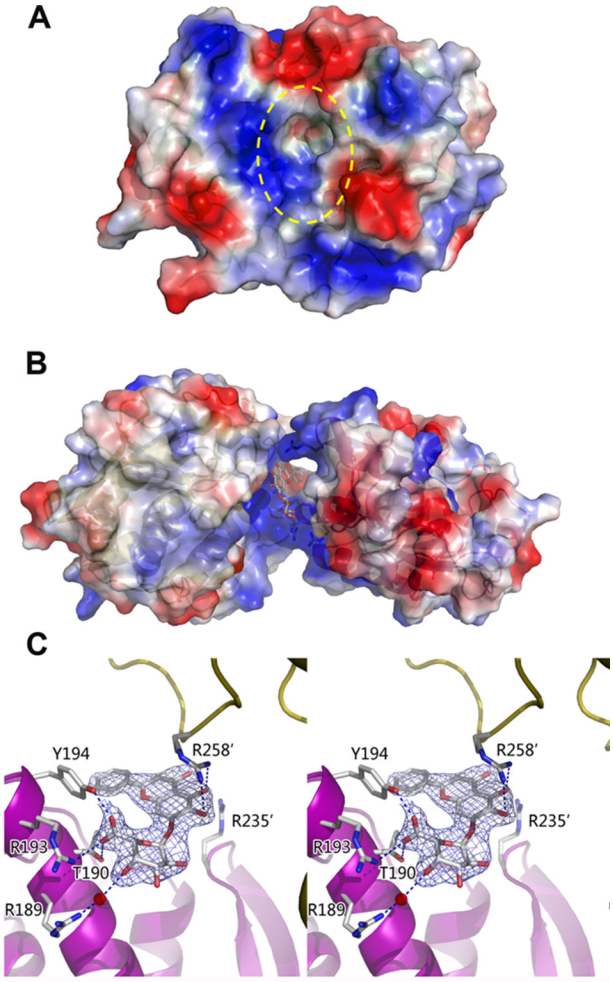

FIGURE 3. **Crystal structure of the baicalin-RTA monomer complex.** *A,* surface representation of RTA monomer (PDB code 1J1M) as the starting model for solving the RTA-BAI complex structure. Positively charged area is colored *blue,* and negatively charged area is in *red*. The *dashed line oval* indicates the active site of the enzyme. *B,* superimposed surface and ribbon representation of two RTA monomers form a pseudo-dimer, which was related by a crystallographic 2_1 helical axis. The BAI inhibitor is represented as ball-and-stick model, which was located at the interface of two RTA monomers. *C,* stereo view of the binding site and the bound BAI molecule. The protein structure is in *ribbon* presentation, with the side chains of amino acid residues interacting with BAI presented in stick style. The $F_o - F_c$ omit electron density map of BAI molecule is superimposed and contoured at 1.0σ (*blue*) with a 1.6 Å radius coverage. Hydrogen bonds were represented as *blue dashed lines,* and the water molecule is represented as a *red ball*.

existence of the BAI molecule at the protein packing interface, which was in great agreement with the structure (Fig. 3*C*). The BAI molecule formed extensive hydrogen bonds with the side chains of 5 of the 6 residues in the binding pocket (Fig. 4). Specifically, the side chain of Thr-190, Arg-193, and Tyr-194 formed hydrogen bonds and ionic bonds with the carboxyl group on the saccharide ring, whereas Arg-189 formed a hydrogen bond with the hydroxyl group of BAI, which is bridged by a bound water molecule. However, Arg-258′ from the other monomer formed two hydrogen bonds with two of the hydroxyl groups on the heterocyclic ring of the BAI molecule (Fig. 3*C*). Although Arg-235 is in the vicinity of the interface between RTA and BAI, it does not appear to participate in hydrogen bond formation.

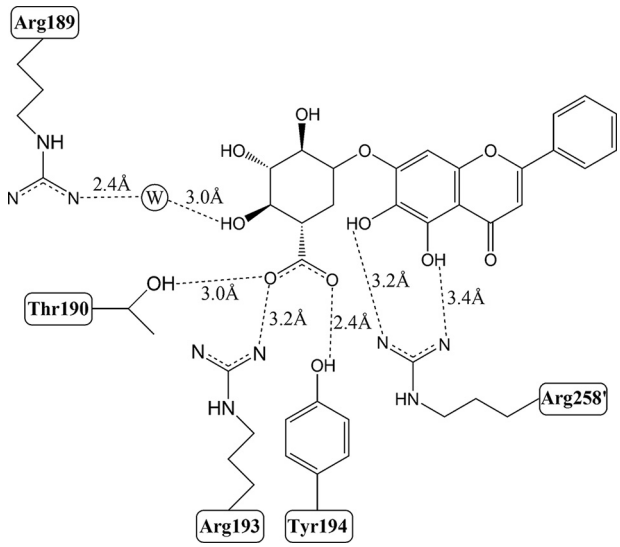

FIGURE 4. **Schematic diagram showing the extensive hydrogen bond network between RTA and baicalin.** Residues of RTA involved in BAI binding are labeled with respective detailed atomic information. Hydrogen bonds are shown as *dashed lines* marked with individual hydrogen bond lengths.

To further analyze the involvement of the several RTA residues in its interactions with BAI, we created mutants of RTA with one of the six residues (Arg-189, Thr-190, Arg-193, Tyr-194, Arg-235, and Arg-258) being replaced with alanine, respectively. None of these mutations significantly affected the potency of the toxin measured by the *in vitro* translation assay (Fig. 5). Interestingly, the R189A, T190A, and R193A mutants had almost completely lost the sensitivity to BAI (Fig. 5). Although still toxic, mutants Y194A, R235A, and R258A still responded to BAI but at detectably lower levels (Fig. 5).

We further examined the interactions between these RTA mutants and BAI by measuring the sedimentation velocity of the complexes using analytical ultracentrifugation. Wild type RTA gave a single peak at the predicted molecular weight, indicating the presence of homogeneous monomeric molecules in the solution (Fig. 6). The addition of BAI to the protein solution caused tailing signals in the ultracentrifugation with a molecular mass as large as 500 kDa, indicative of the presence of heterogeneous toxin oligomers (Fig. 6). Consistent with their insensitivity to BAI, the R189A and R193A mutants maintained their uniform monomeric structure in the presence of BAI (Fig. 6). Minor but readily detectable oligomers can be detected for mutants T190A, Y194A, and R235A in the presence of BAI (Fig. 6), which is consistent with their detectable lower sensitivity to the inhibitor. Instead of directly participating in the interactions, Arg-235 is in the vicinity of the binding pocket; this residue may contribute to the binding indirectly by stabilization of the BAI-binding pocket. BAI induced the formation of a fraction of uniform oligomers by mutant R258A. A less significant but detectable tailing was detected in mutants Y194A, R235A, and R258A (Fig. 6), which is consistent with the loss of sensitivity to BAI by these mutants (Fig. 5). These mutations clearly affect the binding of BAI to ricin, which will inevitably interfere with its ability to induce protein multimerization. Thus, the insensitivity of these mutants to BAI is a result of multiple factors. Taken together, these results suggest that BAI functions by

directly interacting with RTA to induce its oligomerization, thus inactivating its toxicity.

DISCUSSION

Ricin isolated from castor beans poses grave challenges to public health. Because of its high toxicity and the relatively straightforward procedure to obtain large quantities, ricin is a potential bioterrorism agent (29). Thus, there is an urgent need for agents that are clinically effective in treating intoxication caused by these toxins.

Because of the unpredictable nature of ricin poisoning, effective post-exposure therapeutics are considered the most important feature of any agent against this lethal toxin. At least two lines of evidence indicate that baicalin satisfies the requirements as a therapeutic. First, this compound is able to rescue mice from lethal doses of the toxin; second, treatment with baicalin alleviated several pathologies in the animals that are often associated with poisoning caused by ricin. This therapeutic feature distinguishes baicalin from molecules obtained by structural information-based rational design or by cell-based screenings (8, 30), none of which has been demonstrated to be effective as a therapeutic measure. In this regard, baicalin also differs from the several highly reactive, ricin-specific mAbs against ricin developed by Mantis and co-workers (7). These mAbs exhibit high level protection when administered prior to toxin exposure (8, 12, 14), but their effects as therapeutics have not been documented.

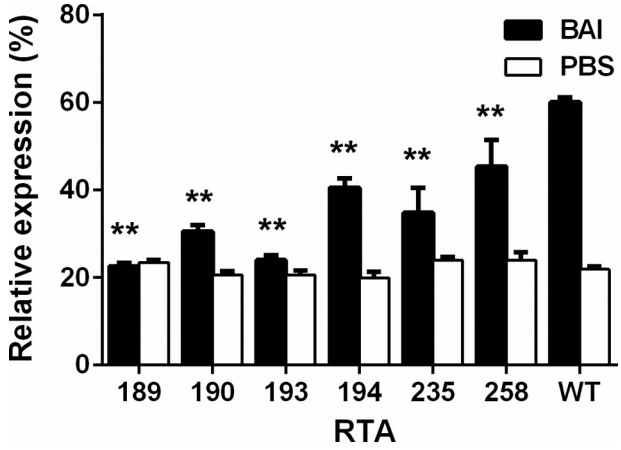

FIGURE 5. **Activity of the RTA mutants in inhibiting protein synthesis.** Purified RTA mutants were measured for their ability to inhibit protein synthesis in a cell-free system; the effects of baicalin were evaluated by including this compound in parallel reactions. The results were expressed as the percentage of control reactions without toxin or baicalin. Note that for RTA, the R189A, T190A, and R193A mutants are no longer responsive to baicalin. All data represent the mean and standard error of three independent experiments. All data represent the mean and standard error of three independent experiments. **, $p < 0.01$.

Ricin opts the retrograde trafficking route to introduce the toxic subunit to the cytosol (5). Blocking the delivery of the toxin to their cellular targets has been exploited to identify agents capable of inhibiting its toxicity. The most exciting progress in this direction was the identification of Retro-1 and Retro-2, two highly selective inhibitors for the transport of ricin to its cellular site of action (18). Importantly, Retro-2 provided significant protection when it was administered within 1 h prior to toxin exposure (18). However, whether this compound is similarly effective in therapeutic post-exposure use remains to be determined.

Many of the known RTA inhibitors against ricin function by blocking its enzymatic activity via occupying the active site. For example, both purine- and pterin-like molecules form complexes with RTA wherein the compound docks into its active site (3, 31). In our study, we also screened several inhibitors that bound to the active site of ricin with *in vitro* activity; however, this type of inhibitor showed no *in vivo* activity in the mouse model. Our structural analysis revealed that rather than occupying the active site of RTA, baicalin exerts its inhibitory effects by inducing the formation of oligomers by the toxin. If the side with the entry of the active site was considered the front of the RTA molecule, baicalin-induced oligomerization appeared to occur by the positioning of the baicalin molecule between two RTA monomers in a "front-to-side" manner (Fig. 3*B*), leading to a propagated oligomerization of RTA by baicalin and blockage of the entry sites of each monomer. Several hydrogen bonds

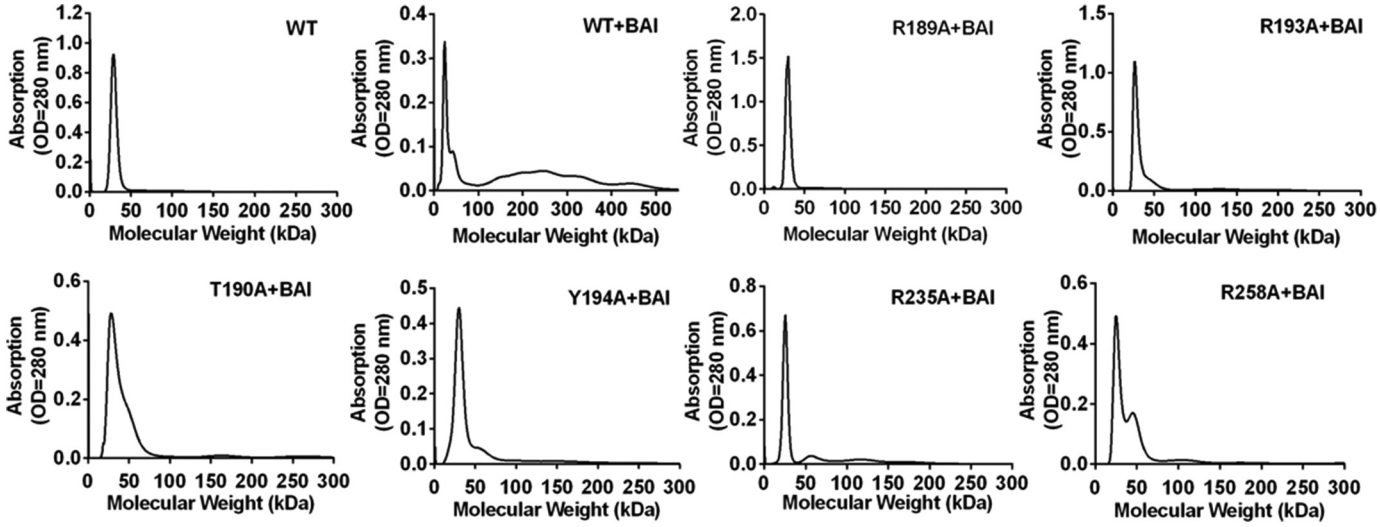

FIGURE 6. **Baicalin-induced formation of oligomers by the mutants.** Solutions containing indicated mutants of RTA and baicalin were subjected to analytical ultracentrifugation to estimate the molecular weight of the samples. Note the presence of almost uniform monomer in samples containing the R189A and R193A mutants.

formed between baicalin and several positively charged RTA surface residues (Arg-189, Thr-190, Arg-193, Tyr-194, Arg-235, and Arg-258) contributed to stabilizing the complex (Figs. 3*C* and 4). None of the residues involved in the binding contributes to the active pocket of the toxin. Predictably, mutations in these residues did not significantly affect the enzymatic activity of the RTA. Thus, the formation of the oligomers obscured the RTA active site, which blocks the access of the substrate, thus leading to lower toxicity. To some extent, the proposed mechanism of action of baicalin is akin to that of mAbs, which abolish the activity of the toxin by forming antibody-toxin complexes (32). Clearly, the sensitivity of the RTA correlated well with the contribution of these residues in the formation of the complex; mutations in residues important for the anchoring of baicalin resulted in mutants that are markedly less responsive to the compound. Thus, our results suggest induction of toxin oligomerization as a novel mechanism of action for neutralizing the toxicity of ricin, which perhaps can be extended to other members of the RIP family.

Chinese herbs have been used for thousands of years for the treatment of many diseases, including infections. Some of these active compounds have been exploited for their anti-virulence property (33, 34). Several questions on the activity and clinical usefulness of baicalin mandate further study. First, baicalin has previously been shown to have anti-inflammatory and anti-tumor activity (33, 35). Whether and how such activities on the host cell contribute to its therapeutic effects remain to be determined. Second, whether baicalin can prevent the lethality of RIP toxins acquired by routes such as infections and nasal exposure remains unknown. Nevertheless, the ability of this compound to therapeutically rescue intoxicated animals represents a significant step forward in our search for agents against these dangerous toxins. From the dosage in the mouse model, the human equivalent dose is predicted to be only about 7 mg/kg according to the standard for human equivalent dose calculation based on body surface area established by the Food and Drug Administration (36). In addition, baicalin does not display significant toxicity to mice at a dose of 15 g/kg (37). These features indicate the low toxicity of baicalin, making it highly acceptable for application in humans. Furthermore, it can be used for further development of more effective compounds against ricin based on the structure and the mechanism of action. Finally, because baicalin and Retro-2 function by completely independent mechanisms, it will be interesting to determine how a combination of these two agents fares in the treatment of ricin intoxication.

REFERENCES

1. Stirpe, F., and Battelli, M. G. (2006) Ribosome-inactivating proteins: progress and problems. *Cell. Mol. Life Sci.* **63,** 1850–1866
2. Endo, Y., Chan, Y. L., Lin, A., Tsurugi, K., and Wool, I. G. (1988) The cytotoxins α-sarcin and ricin retain their specificity when tested on a synthetic oligoribonucleotide (35-mer) that mimics a region of 28 S ribosomal ribonucleic acid. *J. Biol. Chem.* **263,** 7917–7920
3. Miller, D. J., Ravikumar, K., Shen, H., Suh, J. K., Kerwin, S. M., and Robertus, J. D. (2002) Structure-based design and characterization of novel platforms for ricin and shiga toxin inhibition. *J. Med. Chem.* **45,** 90–98
4. Rasooly, R., He, X., and Friedman, M. (2012) Milk inhibits the biological activity of ricin. *J. Biol. Chem.* **287,** 27924–27929
5. Spooner, R. A., and Lord, J. M. (2012) How ricin and Shiga toxin reach the cytosol of target cells: retrotranslocation from the endoplasmic reticulum. *Curr. Top. Microbiol. Immunol.* **357,** 19–40
6. Rapak, A., Falnes, P. O., and Olsnes, S. (1997) Retrograde transport of mutant ricin to the endoplasmic reticulum with subsequent translocation to cytosol. *Proc. Natl. Acad. Sci. U.S.A.* **94,** 3783–3788
7. Mantis, N. J., McGuinness, C. R., Sonuyi, O., Edwards, G., and Farrant, S. A. (2006) Immunoglobulin A antibodies against ricin A and B subunits protect epithelial cells from ricin intoxication. *Infect. Immun.* **74,** 3455–3462
8. Wahome, P. G., Robertus, J. D., and Mantis, N. J. (2012) Small-molecule inhibitors of ricin and Shiga toxins. *Curr. Top. Microbiol. Immunol.* **357,** 179–207
9. Smith, M. J., Melton-Celsa, A. R., Sinclair, J. F., Carvalho, H. M., Robinson, C. M., and O'Brien, A. D. (2009) Monoclonal antibody 11E10, which neutralizes shiga toxin type 2 (Stx2), recognizes three regions on the Stx2 A subunit, blocks the enzymatic action of the toxin *in vitro*, and alters the overall cellular distribution of the toxin. *Infect. Immun.* **77,** 2730–2740
10. Roche, J. K., Stone, M. K., Gross, L. K., Lindner, M., Seaner, R., Pincus, S. H., and Obrig, T. G. (2008) Post-exposure targeting of specific epitopes on ricin toxin abrogates toxin-induced hypoglycemia, hepatic injury, and lethality in a mouse model. *Lab. Invest.* **88,** 1178–1191
11. Neal, L. M., O'Hara, J., Brey, R. N., 3rd, and Mantis, N. J. (2010) A monoclonal immunoglobulin G antibody directed against an immunodominant linear epitope on the ricin A chain confers systemic and mucosal immunity to ricin. *Infect. Immun.* **78,** 552–561
12. Tzipori, S., Sheoran, A., Akiyoshi, D., Donohue-Rolfe, A., and Trachtman, H. (2004) Antibody therapy in the management of shiga toxin-induced hemolytic uremic syndrome. *Clin. Microbiol. Rev.* **17,** 926–941
13. Dowling, T. C., Chavaillaz, P. A., Young, D. G., Melton-Celsa, A., O'Brien, A., Thuning-Roberson, C., Edelman, R., and Tacket, C. O. (2005) Phase 1 safety and pharmacokinetic study of chimeric murine-human monoclonal antibody c α Stx2 administered intravenously to healthy adult volunteers. *Antimicrob. Agents Chemother.* **49,** 1808–1812
14. Bitzan, M., Poole, R., Mehran, M., Sicard, E., Brockus, C., Thuning-Roberson, C., and Rivière, M. (2009) Safety and pharmacokinetics of chimeric anti-Shiga toxin 1 and anti-Shiga toxin 2 monoclonal antibodies in healthy volunteers. *Antimicrob. Agents Chemother.* **53,** 3081–3087
15. Deleted in proof
16. Zhu, Y. W., Dai, J. X., Zhang, T. C., Li, X., Fang, P. F., Wang, H. J., Jiang, Y. L., Yu, X. J., Xia, T., Niu, L. W., Guo, Y. J., and Teng, M. K. (2013) Structural insights into the neutralization mechanism of monoclonal antibody 6C2 against ricin. *J. Biol. Chem.* **288,** 25165–25172; Correction (2013) *J. Biol. Chem.* **288,** 28311
17. Vance, D. J., Tremblay, J. M., Mantis, N. J., and Shoemaker, C. B. (2013) Stepwise engineering of heterodimeric single domain camelid VHH antibodies that passively protect mice from ricin toxin. *J. Biol. Chem.* **288,** 36538–36547
18. Stechmann, B., Bai, S. K., Gobbo, E., Lopez, R., Merer, G., Pinchard, S., Panigai, L., Tenza, D., Raposo, G., Beaumelle, B., Sauvaire, D., Gillet, D., Johannes, L., and Barbier, J. (2010) Inhibition of retrograde transport protects mice from lethal ricin challenge. *Cell* **141,** 231–242
19. Nicolson, G. L., and Blaustein, J. (1972) The interaction of *Ricinus communis* agglutinin with normal and tumor cell surfaces. *Biochim. Biophys. Acta* **266,** 543–547
20. Hale, M. L. (2001) Microtiter-based assay for evaluating the biological activity of ribosome-inactivating proteins. *Pharmacol. Toxicol.* **88,** 255–260
21. Otwinowski, Z., and Minor, W. (1997) Processing of x-ray diffraction data collected in oscillation mode. *Methods Enzymol.* **276,** 307–326
22. McCoy, A. J., Grosse-Kunstleve, R. W., Adams, P. D., Winn, M. D., Storoni, L. C., and Read, R. J. (2007) Phaser crystallographic software. *J. Appl. Crystallogr.* **40,** 658–674
23. Murshudov, G. N., Vagin, A. A., and Dodson, E. J. (1997) Refinement of macromolecular structures by the maximum-likelihood method. *Acta Crystallogr. D Biol. Crystallogr.* **53,** 240–255
24. Adams, P. D., Grosse-Kunstleve, R. W., Hung, L. W., Ioerger, T. R., McCoy, A. J., Moriarty, N. W., Read, R. J., Sacchettini, J. C., Sauter, N. K., and Terwilliger, T. C. (2002) PHENIX: building new software for automated

crystallographic structure determination. *Acta Crystallogr. D Biol. Crystallogr.* **58,** 1948–1954
25. Emsley, P., and Cowtan, K. (2004) Coot: model-building tools for molecular graphics. *Acta Crystallogr. D Biol. Crystallogr.* **60,** 2126–2132
26. Laskowski, R. A., MacArthur, M. W., Moss, D. S., and Thornton, J. M. (1993) PROCHECK: a program to check the stereochemical quality of protein structures. *J. Appl. Crystallogr.* **26,** 283–291
27. Saenz, J. B., Doggett, T. A., and Haslam, D. B. (2007) Identification and characterization of small molecules that inhibit intracellular toxin transport. *Infect. Immun.* **75,** 4552–4561
28. Mlsna, D., Monzingo, A. F., Katzin, B. J., Ernst, S., and Robertus, J. D. (1993) Structure of recombinant ricin A chain at 2.3 A. *Protein Sci.* **2,** 429–435
29. Zhang, J., Qin, D. A., Cheng, B. X., Ru, X. Q., Li, H., Li, L., and Yang, H. P. (1999) Preparation, characteristics and toxicity of ricin-containing galactosyl ceramide liposomes. *Sheng Wu Hua Xue Yu Sheng Wu Wu Li Xue Bao* **31,** 472–474
30. Wahome, P. G., Bai, Y., Neal, L. M., Robertus, J. D., and Mantis, N. J. (2010) Identification of small-molecule inhibitors of ricin and shiga toxin using a cell-based high-throughput screen. *Toxicon* **56,** 313–323
31. Pruet, J. M., Jasheway, K. R., Manzano, L. A., Bai, Y., Anslyn, E. V., and Robertus, J. D. (2011) 7-Substituted pterins provide a new direction for ricin A chain inhibitors. *Eur. J. Med. Chem.* **46,** 3608–3615
32. O'Hara, J. M., Yermakova, A., and Mantis, N. J. (2012) Immunity to ricin: fundamental insights into toxin-antibody interactions. *Curr. Top. Microbiol. Immunol.* **357,** 209–241
33. Qiu, J., Niu, X., Dong, J., Wang, D., Wang, J., Li, H., Luo, M., Li, S., Feng, H., and Deng, X. (2012) Baicalin protects mice from *Staphylococcus aureus* pneumonia via inhibition of the cytolytic activity of α-hemolysin. *J. Infect. Dis.* **206,** 292–301
34. Niu, X., Qiu, J., Wang, X., Gao, X., Dong, J., Wang, J., Li, H., Zhang, Y., Dai, X., Lu, C., and Deng, X. (2013) Molecular insight into the inhibition mechanism of cyrtominetin to α-hemolysin by molecular dynamics simulation. *Eur. J. Med. Chem.* **62,** 320–328
35. Takahashi, H., Chen, M. C., Pham, H., Angst, E., King, J. C., Park, J., Brovman, E. Y., Ishiguro, H., Harris, D. M., Reber, H. A., Hines, O. J., Gukovskaya, A. S., Go, V. L., and Eibl, G. (2011) Baicalein, a component of *Scutellaria baicalensis*, induces apoptosis by Mcl-1 down-regulation in human pancreatic cancer cells. *Biochim. Biophys. Acta* **1813,** 1465–1474
36. Food and Drug Administration (2005) Guidance for Industry, pp. 25–26
37. Zhang, X., and Zhang, Y. (2006) Empirical study on safety and acute toxicity of baicalin injection. *J. Med. Res.* **7,** 16–19

Protein Structure and Folding:

Baicalin Inhibits the Lethality of Ricin in Mice by Inducing Protein Oligomerization

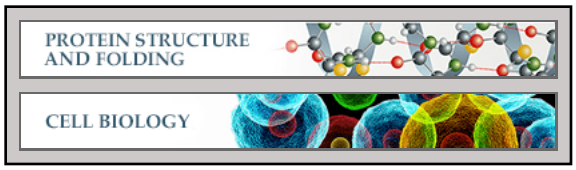

Jing Dong, Yong Zhang, Yutao Chen, Xiaodi Niu, Yu Zhang, Rui Li, Cheng Yang, Quan Wang, Xuemei Li and Xuming Deng

J. Biol. Chem. 2015, 290:12899-12907.
doi: 10.1074/jbc.M114.632828 originally published online April 5, 2015